Raman Spectroscopic Study on Solvation of Diphenylcyclopropenone and Phenol Blue in Room Temperature Ionic Liquids

Tomotsumi Fujisawa,*,† Masanori Fukuda, and Masahide Terazima

Department of Chemistry, Graduate School of Science, Kyoto University, Kyoto, 606-8502, Japan

Yoshifumi Kimura*

Division of Research Initiatives, International Innovation Center, Kyoto University, Kyoto, 606-8501, Japan

Received: December 21, 2005; In Final Form: February 21, 2006

We investigated the solvation of several room temperature ionic liquids by Raman spectroscopy using diphenylcyclopropenone (DPCP) and phenol blue (PB) as probe molecules. We estimated acceptor numbers (AN) of room temperature ionic liquids by an empirical equation associated with the Raman band of DPCP assigned as a C═C stretching mode involving a significant C═O stretching character. According to the dependence of AN on cation and anion species, the Lewis acidity of ionic liquids is considered to come mainly from the cation charge. The frequencies and bandwidths of the C═O and C═N stretching modes of phenol blue are found to be close to those in conventional polar solvents such as methanol and dimethyl sulfoxide. The frequencies of these vibrational modes show similar dependence upon the electronic absorption band center as is observed in conventional liquid solvents. However, peculiar behavior was found in the Raman bandwidths and the excitation wavelength dependence of the C═N stretching mode in room temperature ionic liquids. Both the bandwidth of the C═N stretching mode and the extent of the excitation wavelength dependence of the Raman shift of the C═N stretching mode tend to decrease as the absorption band center decreases, in contrast to the case of conventional solvents. This anomaly is discussed in terms of the properties of room temperature ionic liquids.

1. Introduction

Room temperature ionic liquids (RTILs), which are liquid salts composed of anions and cations at room temperature, have unique properties such as electroconductivity, nonvolatility, and nonflammability, so they are being actively investigated as alternative solvent media in synthesis, catalysis, separations, and electrochemistry.[1−5] Various kinds of ionic liquids have been synthesized and many chemists are engaged in research on them for both academic and technical interests.[6−15] Typical RTILs are composed of a molecular cation with an asymmetrical structure and an anion containing bulky fluorinated groups. The low melting points of RTILs are often ascribed to both the bulky and asymmetrical structure of cation/anion and the charge delocalization over the cation and/or anion. For example, the charge delocalization over the N−C−N portion of the ring in 1,3-dialkylimidazolium cation weakens the electrostatic interaction with the counteranion, and the asymmetrical structure caused by alkyl chains of different length makes for a poor packing of the crystal.

From the physicochemical perspective, it is an important subject to study how the charges of cation/anion, in addition to the structure, affect the bulk properties of the neat liquids and their solvating ability. Various kinds of spectroscopy including Raman spectroscopy and X-ray spectroscopy have been applied to neat RTILs in order to investigate the microscopic structure.[10−13] For example, Hamaguch et al. investigated the structure of imidazolium-based ionic liquids by Raman spectroscopy.[10−13] They found that at least two rotational (trans/gauche) isomers for the alkyl-chain part of the imidalozilum-based cation coexist in RTILs. Further they found that it takes nearly 10 min to reach equilibrium between the trans and gauche conformers in liquid 1-butyl-3-methylimidazolium chloride after melting from the crystalline state. These studies together with the large-angle X-ray scattering data[12] suggested that some locally ordered domains with a probable size of less than 10 nm exist in these RTILs.

Static solvation of RTILs has been investigated by the measurements of well-known empirical solvent parameters such as α, π^*, and $E_T(30)$ values, which are determined by the absorption band peaks of solvatochromic probes.[5,16−19] The values of α and π^* describe the hydrogen bond donating and the dipolarity/polarizability characteristics of solvents, respectively.[20,21] The π^* values of most RTILs are close to unity,[5] which indicates the presence of strong Coulombic interactions between the cation/anion and solute. The $E_T(30)$ value[22] is a very useful solvent parameter for the estimation of gross solvent effects including hydrogen bonding and electrostatic interactions. According to previous studies, $E_T(30)$ values of RTILs cover a wide range between values comparable to those between dimethylformamide (43.8) and water (63.1).[5] The dynamics of solvation in RTILs also has been extensively studied by the measurement of time-dependent fluorescence Stokes shifts (TDFSS).[23−30] A number of studies of TDFSS have shown the presence of slow nanosecond-order solvation dynamics in RTILs, much slower than the times observed in conventional molecular liquids. The slow dynamics has been ascribed to collective translational motions of the cations and anions in the

---

[†] Phone: +81-75-753-4024. Fax: +81-75-753-4000. E-mail: fujisawa@kuchem.kyoto-u.ac.jp.

10.1021/jp057423d CCC: $33.50

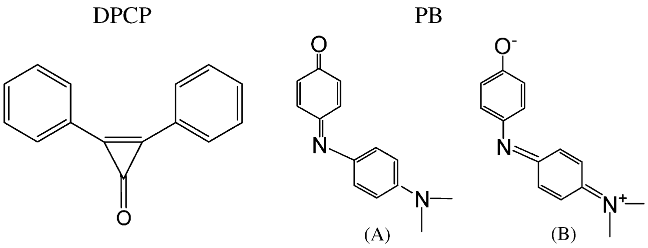

Figure 1. Molecular structures of DPCP, PB: (A) the neutral state and (B) the charge separated state.

viscous solution. One of the interesting findings associated with this slow relaxation is an excitation-wavelength-dependent fluorescence, called “red-edge effect”, of some dipolar solutes in RTILs.[31]

In this paper, we have investigated solvation in RTILs from the viewpoint of the intramolecular structure using vibrational Raman spectroscopy. A solute molecule changes its intramolecular structure as a result of interactions with solvent molecules. The vibrational frequency of particular modes of the solute can be used to monitor intramolecular structure changes. Inhomogeneous broadening of certain vibrational modes is a manifestation of the presence of a distribution of vibrational frequencies caused by fluctuations of interacting solvent molecules around a solute molecule. In this paper, we report studies on diphenylcyclopropenone (DPCP) and phenol blue (PB) as probe molecules. DPCP contains a highly strained cyclopropenone group (Figure 1), and it has been the object of studies of its structure, synthesis, and dissociation dynamics.[32−35] It has been reported that the vibrational frequency of a C=C stretching mode involving a significant C=O stretching character (C=C + C=O stretching mode) shows a large solvent dependence.[36] Santos et al. studied the solvent dependence of this band, and observed a large frequency shift ($\sim$30 cm^{-1}) between the nonpolar solvents and hydrogen-bonding solvents in both Raman and IR spectra.[37] They also made theoretical calculations of dimethylcyclopropenone as a model molecule, and obtained a good agreement between observed and calculated frequencies using a combined SCRF (self-consistent reaction field) with a supermolecule approach. They found that both dielectric and hydrogen bonding properties of the solvent contribute to the band shift. In our previous letter,[38] we reported a good correlation between the vibrational frequency of the C=C + C=O band and the solvent’s acceptor number (AN). This AN is an empirical measure of solvent electrophilicity, which is determined from the chemical shift of ^{31}P NMR of triethylphosphane oxide.[39] The correlation between the band shift of DPCP and AN means that the structure change in DPCP is mainly caused by the electophilicity of the solvent. From the correlation, we estimated the AN values of several RTILs. In the present paper, we discuss the origin of the electrophilicity of RTILs with additional data.

Phenol blue (PB) is a well-known solvatochromic dye and its absorption maximum has been used as a solvent polarity indicator.[40−47] The electronic state of PB is often described by the resonance between two limiting structures, a neutral form (Figure 1A) and a charge-separated form (Figure 1B). The neutral form is dominant in the ground state and the charge-separated form in the excited state. The absorption spectrum of PB shows a large red shift in polar solvents, because the charge-separated electronic excited state is more stabilized by the solvent polarity than the ground state. Yamaguchi et al. extensively studied the absorption and resonance Raman spectra of PB in conventional liquids and in various supercritical fluids.[41−44] They found a linear correlation between the solvatochromic shifts of the electronic absorption and the frequencies and bandwidths of the C=O and C=N stretching modes of PB. The frequencies of these vibrations decrease in the solvents with a larger solvatochromic shift. This frequency shift is interpreted as the result of an increase in the contribution of the charge-separate form to the ground state of PB. It was also shown that the bandwidths, i.e., the fluctuation of the vibrational frequency, are also correlated with the absorption band shift. Furthermore, they found that the Raman shift of the C=N stretching mode is dependent upon the excitation wavelength used for the measurement.[42,43] They interpreted that this dependence as the result of solvation state selective excitation from an inhomogeneous distribution of vibrational states, and explained it based on a Brownian oscillator model.[44] In the present paper, we have measured the absorption and the resonance Raman spectra of PB in RTILs. We have found a correlation between the absorption band center and the vibrational frequencies. The bandwidths of the C=O and C=N stretching modes in RTILs are similar to those observed in conventional liquids, although some peculiarities are noted in RTILs.

2. Experimental Section

2.1. Apparatus. Raman spectra of DPCP and PB were measured at the 90° scattering geometry, using a 64 cm monochromator (Jobin Yvon, T6400) equipped with a CCD detector. The Raman spectra of PB were measured under the resonant condition at various excitation wavelengths. An Ar-ion laser (Coherent, Enterprise; 514.5 nm, 488 nm), a Kr-ion laser (Omnichrome, 643-MRDN-AO1; 568 nm, 647 nm), and a He−Ne laser (JDS Uniphase, 1125P-3352; 633 nm) were used for the excitation. The Raman spectra of DPCP were measured under nonresonant conditions at 514.5 nm. Two different CCD detectors were used, one (Princeton Instrument, Spec-10: 400BXTE) for the shorter wavelength region for excitation wavelengths of 488, 514.5, and 568 nm, and the other (Princeton Instrument, Spec-10:400BRXTE) for the longer excitation wavelengths of 633 and 647 nm. The spectral resolution was about 3 cm^{-1}. The wavelength dependence of the sensitivity of the system was corrected by using the fluorescence intensity of quinine in the shorter wavelength region ($<$570 nm) and *m*-nitro-*N*,*N*-dimethylaniline in the longer wavelength region ($>$600 nm). The absorption spectra were measured with a UV−vis spectrometer (Shimazu UV-2400), and the refractive indexes of RTILs were measured by a refractometer (Erma).

2.2. Materials. DPCP was purchased from Nacalai Tesque and used as received. PB was purchased from Wako Chemicals and used after the purification by recrystallization. Conventional organic solvents (cyclohexane (CHX), ethyl acetate (EtOAc), chloroform ($CHCl_3$), benzene (BZ), dimethyl sulfoxide (DMSO), ethanol (EtOH), methanol (MeOH), 2-propanol (2PrOH)—spectroscopic grade; acetonitrile (ACN), ethylene glycol (EG), 2-butanol (2BuOH)—guaranteed grade) were purchased from Nacalai Tesque, and used as received. We measured the spectra of PB and DPCP in nine different RTILs. Their molecular formulas are shown in Figure 2. Four of these liquids consist of the same cation, 1-butyl-3-methylimidazolium ([BMIM]), and different anions, chloride ([Cl]), hexafluorophosphate ([PF_6]), tetrafluoroborate ([BF_4]), and bis(trifluoromethanesulfonyl)imide ([$(CF_3SO_2)_2N$]). The remaining five are *N*,*N*,*N*-trimethyl-*N*-propylammonium bis(trifluoromethanesulfonly)imide ([$N(Me)_3Pr$][$(CF_3SO_2)_2N$]), *N*,*N*-diethyl-*N*-methyl-*N*-(2-methoxyethyl)ammonium tetrafluoroborate ([$N(Et)_2(Me)(MetOEt)$][BF_4]), *N*,*N*-

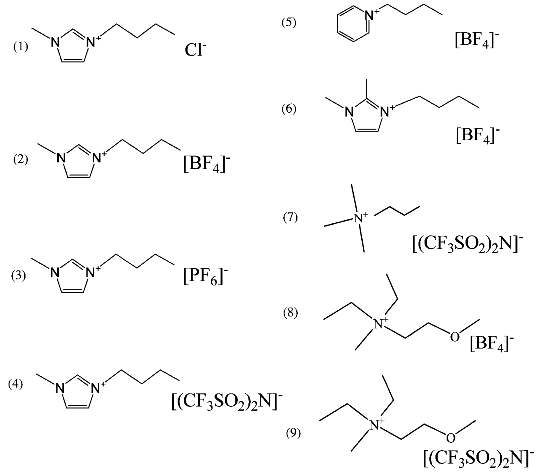

Figure 2. Molecular formulas of RTILs: (1) [BMIM][Cl], (2) [BMIM][BF_4], (3) [BMIM][PF_6], (4) [BMIM][$(CF_3SO_2)_2N$], (5) [BPY][BF_4], (6) [BM_2IM][BF_4], (7) [$N(Me)_3Pr$][$(CF_3SO_2)_2N$], (8) [$N(Et)_2(Me)$(MetOEt)][BF_4], and (9) [$N(Et)_2(Me)$(MetOEt)][$(CF_3SO_2)_2N$].

diethyl-*N*-methyl-*N*-(2-methoxyethyl)ammonium bis(trifluoromethanesulfonyl)imide ([$N(Et)_2(Me)$(MetOEt)][$(CF_3SO_2)_2N$]), 1-butyl-2,3-dimethylimidazolium tetrafluoroborate ([BM_2IM][BF_4]), and 1-butylpyridinium tetrafluoroborate ([BPY][BF_4]). [BMIM][Cl], [BMIM][BF_4] (in part), and [BMIM][PF_6] were synthesized according to refs 48−51 and purified by recrystallization or chromatography. The other seven RTILs were purchased from Kanto Kagaku and used as received. [BMIM][Cl] were in a supercooled state under our experimental conditions. The RTIL solutions were filtered to remove undissolved solute. The concentrations of DPCP and PB were typically 25 and <5 mM (M ≡ mol dm^{-3}), respectively. All measurements were performed at room temperature (23 °C).

It is well-known that a small amount of impurity, especially water, brings a considerable change of some properties of RTILs such as viscosity.[2,3] To eliminate vaporable impurities such as water, all RTILs were evacuated with a vacuum line ($<1.3 \times 10^{-1}$ Pa) more than 30 min before use and a fresh sample was prepared for each measurement. The evacuation process could not completely remove all impurities, since in several RTILs (e.g., [BM_2IM][BF_4] and [BPY][BF_4]) weak fluorescence background signals were observed more or less. The background fluorescence signal was subtracted from the observed spectrum as a smooth baseline, where the baseline function was obtained by fitting the observed spectrum except the Raman bands to a polynomial function of wavelength. The Raman bands due to the solvent were also subtracted by using the Raman spectra from the pure solvents. To test how the water impurity affects the Raman spectrum of PB, we measured the Raman spectrum of PB in a water-added solution of [BMIM][BF_4] (5 vol % of water). Surprisingly there was no change in the Raman spectra of PB by adding water. This is probably because PB is water insoluble and no preferential solvation of water occurs around PB. Similarly, the effect of water on the Raman spectrum of DPCP is expected to be small, since DPCP is also insoluble to water.

3. Results and Discussion

3.1. Raman Spectra of DPCP in RTILs and the Origin of Lewis Acidity of RTILs. Figure 3 shows Raman spectra of DPCP in various solvents measured under the nonresonant conditions at 514.5 nm. As is mentioned in the Introduction, the band assigned to the C═C + C═O mode of DPCP (around 1642 cm^{-1} in CHX) shows drastic solvent dependence. In the previous letter,[38] we reported a good correlation between the frequency of the C═C + C═O band and the acceptor number (AN) in conventional solvents as is shown in Figure 4. This correlation can be expressed by

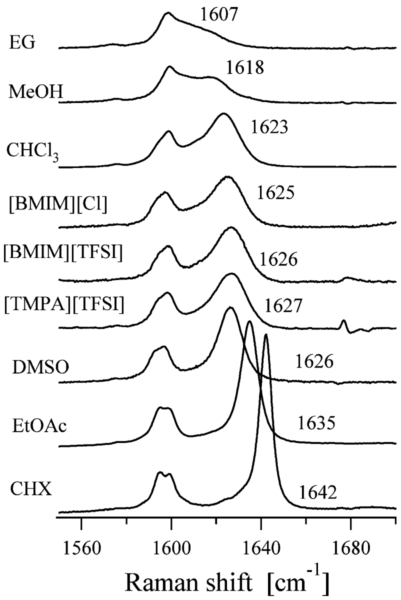

Figure 3. Raman spectra of DPCP in various solvents. The numbers are the peak positions of the C═C + C═O band estimated from the fitting to the Gaussian functions.

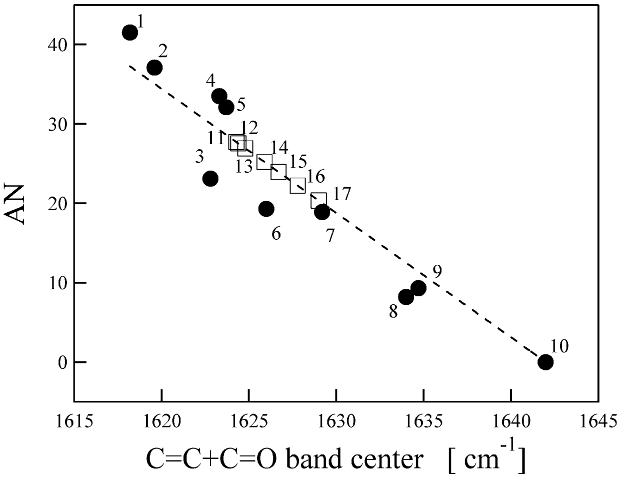

Figure 4. The correlation between AN and the band center of the C═C + C═O band of DPCP in various solvents. The dashed line is the linear least-squares fitting for conventional molecular solvents 1−10. The AN values of RTILs are calculated from the fitting: (1) MeOH, (2) EtOH, (3) $CHCl_3$, (4) 2-PrOH, (5) 2-BuOH, (6) DMSO, (7) ACN, (8) BZ, (9) EtOAc, (10) CHX, (11) [BMIM][PF_6], (12) [BM_2IM][BF_4], (13) [BMIM][BF_4] and [BMIM][Cl], (14) [BMIM][$(CF_3SO_2)_2N$], (15) [$N(Et)_2(Me)$(MetOEt)][BF_4], (16) [$N(Me)_3Pr$][$(CF_3SO_2)_2N$], and (17) [$N(Et)_2(Me)$(MetOEt)][$(CF_3SO_2)_2N$].

$$\mathrm{AN} = 1.565(1642 - \nu/\mathrm{cm}^{-1}) \qquad (1)$$

where ν is the wavenumber of the band center. With increasing electrophilicity or Lewis acidity of the solvent, solvent interactions with the oxygen atom of DPCP weaken the C═O bond. The AN value of RTIL studied here ranges from 20 to 30, and the values are generally smaller than those estimated from the relation between AN and $E_T(30)$ values.[52] The estimated AN values of RTILs are listed on Table 1 with those of typical conventional solvents.

TABLE 1:

solvent	AN	E_{PB}(exptl)/kcal·mol^{-1}	α	π*	E_{PB}(calcd)/kcal·mol^{-1}	*n*
MeOH	41.5^a	47.0	0.93^d	0.6^d	47.0	1.330
DMSO	19.3^a	47.4	0^d	1^d	47.6	1.479
$CHCl_3$	23.1^a	48.1	0.22^e	0.76^e	48.0	1.447
CHX	0^{a,b}	51.8	0^d	0^d	51.8	1.427
BZ	8.2^a	49.9	0^d	0.59^d	49.3	1.474
EtOAc	9.3^a	50.1	0^d	0.55^d	49.5	1.373
EG		45.1	0.9^d	0.92^d	45.7	1.427
[BMIM][PF_6]	27.7	47.7	0.634^f	1.032^f	46.6	1.410
[BMIM][BF_4]	26.9	47.5	0.627^f	1.047^f	46.6	1.423
[BMIM][$(CF_3SO_2)_2N$]	25.2	47.9	0.617^f	0.984^f	46.8	1.426
[BM_2IM][BF_4]	27.5	47.4	0.402^f	1.083^f	47.4	1.434
[BPY][BF_4]	*c*	47.4				1.445
[$N(Me)_3Pr$][$(CF_3SO_2)_2N$]	22.2	48.5				1.403
[BMIM][Cl]	26.9	46.7				1.509
[$N(Et)_2(Me)(MetOEt)$][BF_4]	23.9	47.7				1.408
[$N(Et)_2(Me)(MetOEt)$] [$(CF_3SO_2)_2N$]	20.3	48.6				1.416

[a] Reference 52. [b] Reference 53. [c] Reference 54. [d] Reference 58. [e] Reference 57. [f] Reference 16.

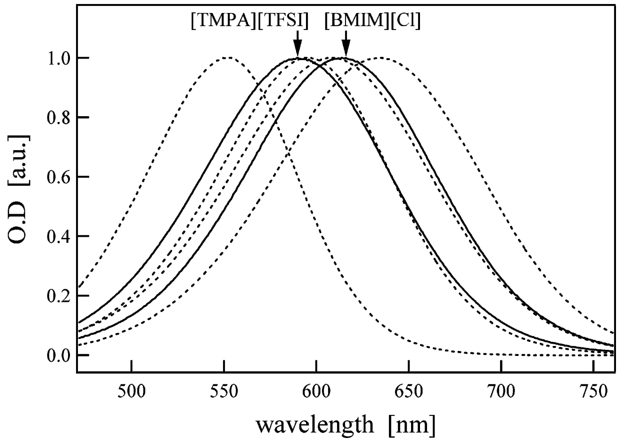

Figure 5. Absorption spectra of PB in some conventional molecular solvents and RTILs. Dotted lines: from left to right, CHX, $CHCl_3$, MeOH, EG. Solid lines: left, [$N(Me)_3Pr$][$(CF_3SO_2)_2N$]; right, [BMIM]-[Cl].

With respect to the dependence of the anion species, the variation of AN is small despite a large anion size change from [BMIM][Cl] to [BMIM][$(CF_3SO_2)_2N$]. It is known that there is a considerable charge localization on the oxygen atom in DPCP.[32] We consider that the electrophilicity of RTILs mainly comes from the positive charge of a cation. Probably because the oxygen atom is predominantly solvated by the cation species, counteranions cannot interact with the C═O bond. This is considered to be the reason the C═C + C═O vibrational frequency is insensitive to anion species.

It is to be noted that RTILs composed of alkylammonium cations show significant Lewis acidities comparable to those of [BMIM]. Considering that the AN value of triethylamine is only 1.4, the large AN value of alkylammonium-based RTILs is due to the charges in solution characteristic to RTILs. It is also noted that the AN value of [BM_2IM][BF_4] is close to that in [BMIM][BF_4]. It is often suggested that the 2-H proton in the imidazolium ring has a hydrogen-donating ability, and that it plays an important role in solvation.[5,16,55,56] However, our result suggests that the Lewis acidity of the [BMIM][BF_4] is not necessarily related to the 2-H proton, and that the other ring protons or the positive charge of the imidazolium ring, as a whole, is important.

Within the same cation group ([BMIM]), the AN values show a slight decrease in the order of [PF_6] > [BF_4] > [$(CF_3SO_2)_2N$]. It is to be noted here that a similar dependence on the anion species is observed in the ionicity of the ionic liquids defined as the ratio (Λ_{imp}/Λ_D) of the conductivity (Λ_{imp}) to the calculated conductivity from the diffusion coefficients (Λ_D).[61] Watanabe et al. have investigated the ratio extensively in varieties of RTILs, and suggested that the ionicity represents the extent of the association between cation and anion in RTILs.[61] It is reasonable that the values of AN are small in RTILs with small values of ionicity due to the larger extent of ionic association. In such a case, the solvation due to the cation is expected to be less effective, because of the ionic pair formation between cation and anion.

3.2. Absorption Spectra of PB. The absorption spectra of PB in conventional liquids and two RTILs are shown in Figure 5. The absorption band peak positions are located at the lower energy side in polar or protic conventional solvents such as MeOH and EG. Among RTILs used here, the absorption band in [BMIM][Cl] ([$N(Me)_3Pr$][$(CF_3SO_2)_2N$]) shows the largest red shift (blue shift). Generally, the peak positions in RTILs are similar to those in MeOH, DMSO, and $CHCl_3$. However, an empirical relation that connects the absorption peak of PB with other solvent polarity parameters suggests that the origin of the spectrum shift may be different among these solvents. The absorption peak energy of PB (E_{PB}/kcal·mol^{-1}) is given as[57]

$$E_{PB}/\mathrm{kcal{\cdot}mol}^{-1} = 51.82 - 4.26\pi^* - 2.46\alpha \qquad (2)$$

According to eq 2, the absorption peak of PB is about 1.7 (4.26/2.46) times more sensitive to Coulombic interactions (π*) than to hydrogen bond acidity (α). Table 1 shows the values of E_{PB} calculated from the π* and α values (E_{PB}(calcd)) together with the experimental values (E_{PB}(exptl)). Generally eq 2 reproduces the experimental value well, although calculated values for RTILs are somewhat smaller than the observed values except for [BM_2IM][BF_4]. Since the π* values of RTILs are large (∼1), the dipolarity/polarizability effect is the main contribution to the shift of PB in RTILs. Although the dipolarity/polarizablity effect is usually affected by the molecular structure of the solvent, π* values of most RTILs are reported to be about 1 irrespective of their molecular structures.[5] Therefore, we consider that the large π* values of RTILs come from the charges of anion and cation rather than dipoles which originate from the charge distribution within cation or anion molecules. As is observed in the case of DPCP, the absorption frequency in [BM_2IM][BF_4] is close to the frequency in [BMIM][BF_4] although the 2-H proton of the imidazolium ring is reported to have significant hydrogen bond ability.[5,16,55,56] This result also indicates that the 2-H proton does not play a special role from the viewpoint of the spectroscopy.

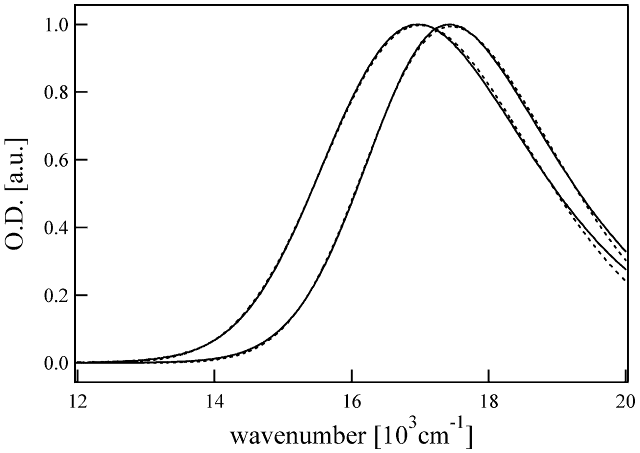

Figure 6. Example of the fitted spectra: left, MeOH; right, $[N(Me)_3Pr][(CF_3SO_2)_2N]$. The observed and the fitted spectra are drawn by the solid and the broken lines, respectively.

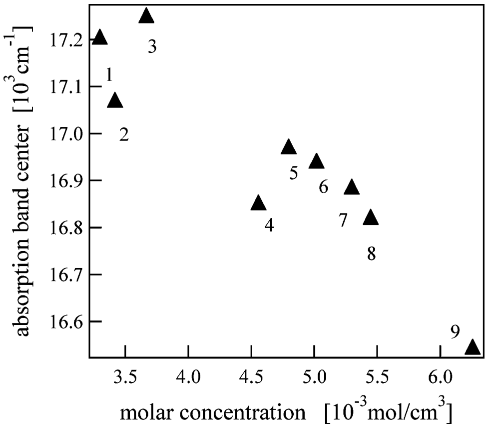

Figure 7. The correlation between the molar concentration of RTILs and the absorption band center ω_0: (1) $[N(Et)_2(Me)(MetOEt)][(CF_3SO_2)_2N]$, (2) $[BMIM][(CF_3SO_2)_2N]$, (3) $[N(Me)_3Pr][(CF_3SO_2)_2N]$, (4) $[BM_2IM][BF_4]$, (5) $[BMIM][PF_6]$, (6) $[N(Et)_2(Me)(MetOEt)][BF_4]$, (7) $[BMIM][BF_4]$, (8) $[BPY][BF_4]$, and (9) [BMIM][Cl].

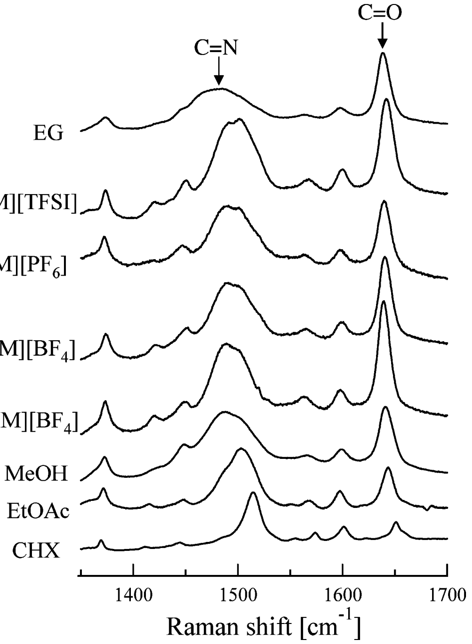

Figure 8. Raman spectra of PB in some conventional molecular solvents and RTILs. Solvent bands are subtracted from the observed spectra except for the case in MeOH.

To make a comparison with the previous analysis of PB by Yamaguchi et al.,[41] we have analyzed the absorption band by a model where the electronic potentials are described by the displaced harmonic wells with one typical intramolecular harmonic vibrational mode. In this model, the absorption band shape is given by[59]

$$\epsilon/\omega \propto \frac{\exp(-\lambda_V/\omega_V)}{\sqrt{4\pi kT\lambda_S}} \sum_{n=0}^{\infty} \frac{(\lambda_V/\omega_V)^n}{n!} \exp\left[-\frac{\{\omega - (\lambda_S + \Delta G + n\omega_V)\}^2}{4\lambda_S kT}\right] \quad (3)$$

where ϵ, ΔG, λ_S, ω_V, and λ_V are the molecular absorption coefficient, the free energy gap between the ground and excited electronic states, the solvent reorganization energy, the intramolecular vibrational frequency, and the intramolecular vibrational reorganization energy, respectively. The first-order and the second-order cumulants of the spectral line shape function, respectively, are given by

$$\omega_0 = \Delta G + \lambda_S + \lambda_V \quad (4)$$

$$\sigma^2 = 2kT\lambda_S + \omega_V\lambda_V \quad (5)$$

which stand for the center and the squared width of the spectrum, respectively.

We have fitted the absorption spectrum of PB in RTILs to eq 3 to obtain ω_0 and σ^2. Fitting parameters are λ_S, λ_V, and ΔG. In these fits, we fixed ω_V to be 1500 cm^{-1} as was done by Yamaguchi et al.[41] Example fits are shown in Figure 6. Some deviation between the observed and fitted spectra on the blue edge is considered to be mainly due to overlap with the S_0-S_2 absorption. From the parameters obtained by the fitting, we calculated ω_0 and σ^2 from eqs 4 and 5. In this paper, we focus mainly on ω_0 and discuss the relationship of the vibrational frequency and bandwidth.

Before the discussion on the relationship of ω_0 with the vibrational structure of PB, we will consider the factor that affects ω_0 among various RTILs. A relatively good correlation is found between ω_0 and the molar concentration of RTILs (Figure 7). The molar concentrations of RTILs are taken from literature.[60−66] As is seen from Figure 7, ω_0 decreases with an increase of the molar concentration of RTILs, i.e., the charge density seems to mainly contribute to stabilization of the charge-separated excited state of PB in RTILs. It is very interesting that the molar concentrations of RTILs are much smaller than those of conventional molecular liquids such as MeOH, $CHCl_3$, and DMSO although the values of ω_0 are close. For example, ω_0 values in $CHCl_3$ and DMSO are very close to those in $[BMIM][(CF_3SO_2)_2N]$ and $[BPY][BF_4]$, respectively. However, the molar concentrations of $CHCl_3$ and DMSO are 13×10^{-3} and 14×10^{-3} mol cm^{-3}, respectively, which are much larger than those of $[BMIM][(CF_3SO_2)_2N]$ (3.4×10^{-3} mol cm^{-3}) and $[BPY][BF_4]$ (5.2×10^{-3} mol cm^{-3}). This indicates that the solvent field of a cation/anion pair is stronger than one molecule of conventional solvents, so the former stabilizes the excited state and decreases ΔG more than the latter.

3.3. Intramolecular Structure Change of PB in RTILs.

The resonance Raman spectra of PB in conventional molecular solvents and RTILs obtained by 514.5 nm excitation are shown in Figure 8. According to ref 41, the characteristic bands around 1500 and 1640 cm^{-1} are assigned to C=N and C=O stretching

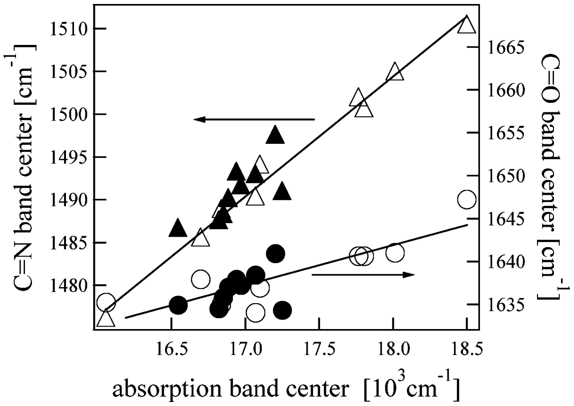

Figure 9. C=O and C=N vibrational frequencies vs absorption band center ω_0 in various conventional molecular solvents (open symbols) and in RTILs (filled symbols). Solid lines are the linear least-squares fits of the conventional solvent data.

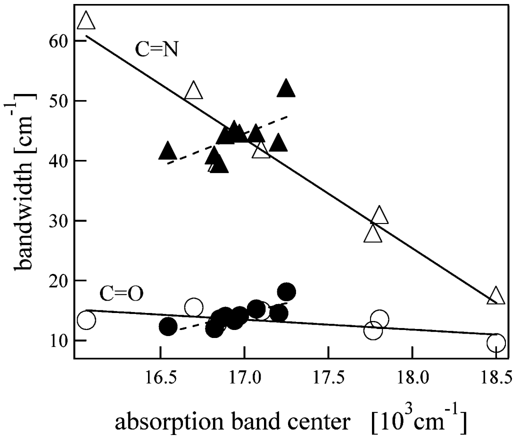

Figure 10. C=O and C=N bandwidths vs absorption band center ω_0 in conventional molecular solvents (open symbols) and in RTILs (filled symbols). The solid and dashed lines are linear least-squares fits of the data of the conventional solvents and RTILs, respectively.

modes, respectively. The positions, bandwidths, and relative intensities of these bands vary considerably with solvents. Figure 9 shows a plot of the peak positions determined by the spectrum fitting to a Gaussian function against the absorption band center ω_0. Although some minor bands overlap the C=N band, we have fitted the whole band to a Gaussian function because the band decomposition was very difficult and the contributions of other bands were small.[41] It is found that both Raman bands have a tendency to shift to lower frequencies as ω_0 decreases. The C=N stretching band peak and the absorption band center are especially well correlated. As is mentioned in the Introduction, the ground state of PB is represented by a resonance between two limiting structures, a neutral form and a charge separated form. In more polar solvents (small ω_0), the charge separated form contributes to the ground state more than in nonpolar solvents. This structural change weakens the C=O and C=N bonds, which results in a shift of both bands to lower frequency. The correlation between the Raman shift and ω_0 in RTILs (filled symbols in Figure 9) is almost the same as that in conventional solvents (open symbols in Figure 9). This indicates that the structure of PB in RTILs is close to that in conventional molecular solvents with a comparable value of ω_0.

3.4. Solvent Fluctuation of RTILs around PB. *3.4.1. Raman Bandwidth.* As is mentioned in the Introduction, the bandwidths of the C=N and C=O modes of PB reflect the fluctuations of solute−solvent interactions. Figure 10 shows a plot of the C=O and C=N bandwidths against the absorption band center ω_0.

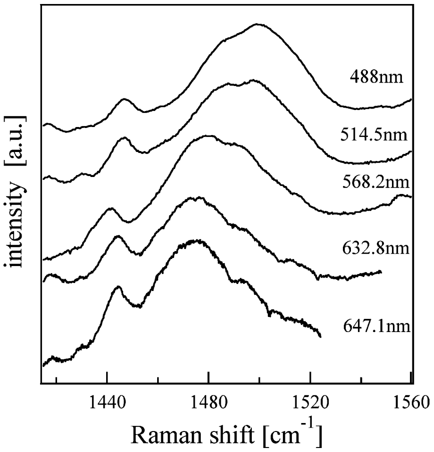

Figure 11. Excitation wavelength dependence of the C=N stretching band of PB in [BMIM][(CF$_3$SO$_2$)$_2$N] solution. The numbers in the figure are the excitation wavelengths.

As is seen from Figure 10, both bandwidths (C=N and C=O) become broader as ω_0 decreases (solid lines). This trend is reasonable considering that strong solute−solvent interactions which decrease ΔG generally accompany a large modulation of the bond frequency due to the solvent fluctuation. The bandwidths in RTILs are also roughly the same as those in conventional molecular liquids with comparable ω_0; i.e., the fluctuation of the solute structure in RTILs is close to that in conventional solvents with comparable ω_0. However, it is noted that the bandwidths in RTILs seem to have a different trend from that in conventional molecular solvents; i.e., the bandwidths in RTILs seem to become narrow with a decrease of ω_0 (dashed lines in Figure 10). To analyze this point further, we measured the excitation wavelength dependence of the frequency of the C=N stretching mode, which will be discussed in the next section.

3.4.2. Excitation Wavelength Dependence of the Raman Shift of the C=N Stretching Mode of PB. Yamaguchi et al. reported that the peak position of the C=N stretching mode of PB depends on the excitation wavelength in polar or protic solvents.[42,43] The phenomenon was ascribed to the solvation state selective excitation from inhomogeneously distributed vibrational states, and confirmed by theoretical model calculations.[44] An important prediction from the theoretical calculation was that two conditions are satisfied to observe such dispersion of resonance Raman frequencies with the excitation wavelength: there must be a correlation between the fluctuations in electronic and vibrational energies, and the vibrational dephasing time must be faster than the relaxation time of the solvent. Briefly, when the solvent motion is slow and almost stopped in the time scale of the resonance Raman scattering process, each resonant wavelength selects a differently solvated molecule among inhomogeneously distributed solvation states. This results in a frequency dispersion with the excitation wavelength.

In RTILs, we have observed similar changes in the Raman band shift with the excitation wavelength. Figure 11 shows the case in [BMIM][(CF$_3$SO$_2$)$_2$N]. The C=N band moves to the lower frequency as the excitation wavelength increases. The peak positions of the C=N stretching mode of PB in some RTILs are plotted against the frequency of the excitation wavelength in Figure 12. Roughly speaking, the change of the Raman shift in RTILs is similar to that in MeOH ($\sim$26 cm^{-1}) and DMSO ($\sim$12 cm^{-1}).[43] As is mentioned in the previous section, the excitation wavelength dependence may be observed only when there is a correlation between the electronic and

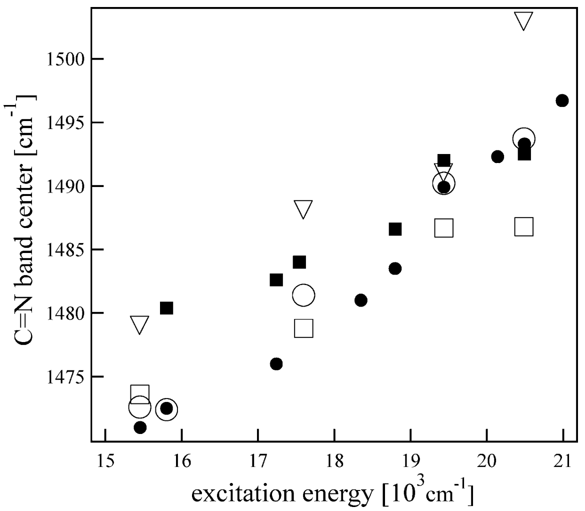

Figure 12. C═N peak positions of PB plotted against the excitation frequency: □, in [BMIM][Cl]; ○, in [BMIM][BF_4]; ▽, in [N(Me)$_3$Pr]-[(CF_3SO_2)$_2$N]; ●, in MeOH, and ■, in DMSO. The data in the conventional solvents (MeOH and DMSO) are taken from ref 39.

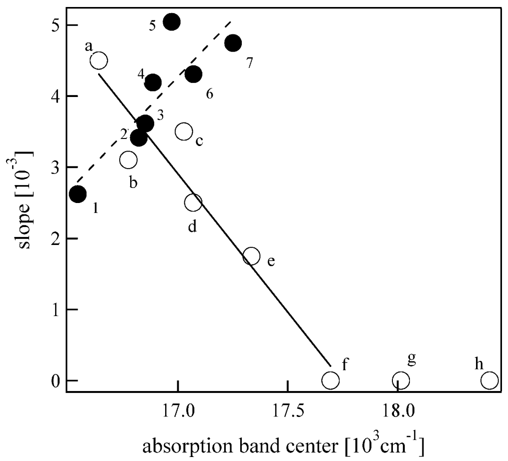

Figure 13. The slopes of the excitation wavelength dependence of the C═N vibrational frequencies of PB in RTILs (filled) and various conventional solvents (open) are plotted against absorption band center. The data in the conventional solvents are taken from ref 42. The solid line is the linear fit for the data in the conventional solvents (a−f) and dashed line in RTILs: (1) [BMIM][Cl], (2) [BPY][BF_4], (3) [BM_2IM]-[BF_4], (4) [BMIM][BF_4], (5) [BMIM][PF_6], (6) [BMIM][(CF_3SO_2)$_2$N], and (7) [N(Me)$_3$Pr][(CF_3SO_2)$_2$N]; (a) MeOH, (b) $CHCl_3$, (c) DMSO, (d) dimethylformamide, (e) ACN, (f) BZ, (g) carbon tetrachloride, and (h) CHX.

vibrational transitions and the solvent relaxation time is slower than the vibrational dephasing time. As is shown in Sections 3.3 and 3.4.1, both the vibrational frequency and bandwidth of the C═N stretching mode are correlated with the absorption band center ω_0. According to the studies with TDFSS,[23−30] the solvent relaxation of RTILs around the dipolar solute shows a complex response with more than two time constants: the faster decay within a few picoseconds, and the longer decays extend into the nanoseconds range. Since the dephasing time is expected to be less than a picosecond, the frequency change in RTILs reflects the local inhomogeneity around the C═N bond. Consistently, the C═N bandwidths in RTILs are close to those in MeOH and DMSO.

To explore the differences among the RTILs, we use the average slope of the C═N frequency change with excitation frequencies as the measure of inhomogeneity of the C═N bond. These slopes are plotted against the absorption band center in Figure 13. It is noted that the slope in RTILs decreases with a decrease of ω_0 (dashed line). In the conventional liquids, the slope increases with an increase of ω_0 (solid line),[43] which is expected from the ordinary relationship between the Raman bandwidth and the absorption band center ω_0. The inverse correlation in the case of RTILs is consisitent with the inverse relationship between the C═N bandwidth and ω_0 observed in RTILs.

Usually, the extent of the structural fluctuation of a solute increases with an increase of the solvent reaction field induced by the solute dipole moment.[39] If the shift of the absorption band center ω_0 represents the solvent reaction field, a large structural fluctuation in the solvent with small ω_0 is observed as a broad Raman bandwidth or the large dispersion with excitation frequency. This is true for the C═N and C═O bands in conventional molecular solvents. However, in RTILs, an inverse dependence of the vibrational fluctuation on ω_0 is observed.

We consider two plausible origins of this anomaly. One is that the shift of ω_0 within RTILs does not reflect the difference of solvent fluctuation. According to eq 4 the absorption band center is a sum of ΔG, λ_S, and λ_V. The free energy difference ΔG is not determined only by the solvent reorganization energy but also by the polarizability response of the solvent, which is not reflected in fluctuation.[39] If the effect due to the polarizability makes a significant contribution to the spectrum shift, the solvent fluctuation may not correlate with ω_0. In fact, it has been reported that the bandwidth of the C═N stretching mode in supercritical CF_3H is extraordinarily larger than is expected from the correlation with ω_0 in conventional liquids.[41] The reason is ascribed to the relatively small shift of ω_0 due to the small refractive index of CF_3H, which represents the strength of the reaction field from the solvent polarizability. In the present case, the refractive index of [BMIM][Cl] is slightly high (Table 1). Therefore, the bandwidth of the C═N band may be smaller than expected from the correlation with ω_0.[68] However, the refractive indices of RTILs, except for [BMIM][Cl], are similar and another effect may exist for the decrease of the fluctuation with decreasing the absorption band center in RTILs.

Another possibility is the saturation of the solvation around the solute. When a favorable solvation structure is present in a RTIL solution caused by interactions between the dipole of the solute and the charges of ions, the solvent fluctuation around the solute may be suppressed. Associated with this idea, the effect of an anion size is considered to be important. An anion with a small size, such as Cl^-, can get close to the solute and interact strongly. At the same time, a small anion also strongly interacts with the countercation. These interactions may suppress the fluctuation of ions. On the other hand, an anion with a large size has a space that enables various configurations and the electrostatic interaction becomes weak, which may lead to flexible solvent configurations. Actually, the slope of the C═N bond frequency change with the excitation wavelength is small (large) in RTILs with a small (large) anion, such as [Cl^-] ([PF_6] and [(CF_3SO_2)$_2$N]). As is mentioned in the Introduction, Hamaguchi et al. observed unusually long equilibration time between the trans and gauche conformers for liquid [BMIM]-[Cl].[11,13] They ascribed this to the relaxation equilibrium between the locally ordered domain and the disordered domain. This locally ordered character of [BMIM][Cl] could be related to the rigidity of the solvation shell and result in the narrowing of the Raman bandwidth (Figure 10) and the smaller C═N frequency change (Figure 13) with a decrease of ω_0.

4. Conclusion

We investigated solvation properties of RTILs by Raman spectroscopy using DPCP and PB as probe molecules. Using the vibrational band of the C═C + C═O mode of DPCP, we have determined the AN values of various RTILs. The AN values are in a range between 20 and 30, smaller than the values predicted from the relation between $E_T(30)$ and AN. Our results suggest that the electrophicilicty of RTILs mainly comes from the positive charge of the cation rather than from the H-bond interactions.

The absorption band peaks of PB in RTILs are similar to those of conventional polar solvents, including DMSO, $CHCl_3$, and MeOH. The Coulombic interaction between PB and RTILs is the main determinant of the absorption peak position. We also found that the absorption band center decreases with an increase of molar concentration in RTILs. This observation indicates that the charge concentration mainly contributes to the stabilization of the charge separated excited state of PB. On the basis of the frequencies of the C═N and C═O Raman bands of PB, we find that the change of the solute structure in RTILs is comparable to what is found in conventional solvents. The fluctuation of the vibrational frequency in RTILs shows the different dependence on ω_0 from that of conventional solvent. Although the Raman bandwidths of the C═N and C═O bands in RTILs are close to those in conventional polar solvents, the dependence on the absorption band center seems to be opposite that of conventional solvents. The dependence of C═N frequency change in RTILs with the excitation wavelength on the absorption band center is similar to the case of the Raman bandwidths. This anomalous trend is considered to come partially from the difference in the refractive indices of various RTILs and partially from enhanced rigidity in RTILs with a decrease of the absorption band center.

Acknowledgment. This work is supported by Grants-in-Aid for Scientific Research from JSPS (Nos. 16350010 and 17073012). We are grateful to Prof. M. Maroncelli (Pennsylvania State University) for fruitful discussions. We are grateful to Prof. O. Kajimoto (Kyoto University) for the kind offer of the spectromator.

References and Notes

(1) Welton, T. *Chem. Rev.* **1999**, *99*, 2071.

(2) *Ionic liquids: The Front and Future of Material Development*; Ohno, H., Ed.; CMC: Tokyo, Japan, 2002.

(3) *Ionic Liquids in Synthesis*; Welton, T., Ed.; Willy−VCH−Verlag: Weinheim, Germany, 2003.

(4) Buzzeo, M. C.; Evans, R. G.; Compton, R. G. *ChemPhysChem.* **2004**, *5*, 1106.

(5) Poole, C. F. *J. Chromatogr. A* **2004**, *1037*, 49.

(6) Ue, M.; Takeda, M.; Toriumi, A.; Kominato, A.; Hagiwara, R.; Ito, Y. *J. Electrochem. Soc.* **2005**, *150* (4), A499.

(7) Weingartner, H.; Knocks, A.; Schrader, W.; Kaatze, U. *J. Phys. Chem. A* **2001**, *105*, 8646.

(8) Paul, A.; Mandal, P. K.; Samanta, A. *Chem. Phys. Lett*. **2005**, *402*, 375.

(9) Liu, J.; Jonsson, J. A.; Jiang, G. *Trends Anal. Chem.* **2005**, *24*, 20.

(10) Ozawa, R.; Hayashi, S.; Saha, S.; Kobayashi, A.; Hamaguchi, H. *Chem. Lett.* **2003**, *32*, 948.

(11) Hamaguchi, H.; Ozawa, R.; Hayashi, S.; Satyen, S. *Abstract of Papers*, 226th National Meeting of the American Chemical Society; American Chemical Scoiety: Washington, DC, 2003; U622.

(12) Katayanagi, H.; Hayashi, S.; Hamaguchi, H.; Nishikawa, K. *Chem. Phys. Lett.* **2004**, *392*, 460.

(13) Hamaguchi, H.; Ozawa, R. *Adv. Phys. Chem.* **2005**, *131*, 85.

(14) Hyun, B. R.; Dzyuba, S. V.; Bartsch, R. A.; Quitevis, E. L. *J. Phys. Chem. A* **2002**, *106*, 7579.

(15) Valkenburg, M. E. V.; Vaughn, R. L.; Williams, M.; Wilkes, J. S. *Thermochim. Acta* **2005**, *425*, 181.

(16) Crowhurst, L.; Mawdsley, P. R.; Perez-Arlandis, J. M.; Slater, P. A.; Welton, T. *Phys. Chem. Chem. Phys.* **2003**, *5*, 2790.

(17) Fletcher, K. A.; Storey, I. A.; Hendricks, A. E.; Pandey, S.; Pandey, S. *Green Chem*. **2001**, *3*, 210.

(18) Baker, S. N.; Baker, G. A.; Bright, F. V. *Green Chem*. **2002**, *4*, 165.

(19) Dzyuba, S. V.; Bartsch, R. A. *Tetrahedron Lett*. **2002**, *43*, 4657.

(20) Taft, R. W.; Kamlet, M. J. *J. Am. Chem. Soc.* **1976**, *98*, 2886.

(21) Kamlet, M. J.; Abboud, J. L.; Taft, R. W. *J. Am. Chem. Soc.* **1977**, *99*, 6027.

(22) Reichardt, C. *Chem. Rev.* **1994**, *94*, 2319.

(23) Karmakar, R.; Samanta, A. *J. Phys. Chem. A* **2002**, *106*, 6670.

(24) Karmakar, R.; Samanta, A. *J. Phys. Chem. A* **2002**, *106*, 4447.

(25) Saha, S.; Mandal, P. K.; Samanta, A. *Phys. Chem. Chem. Phys*. **2004**, *6*, 3106.

(26) Chowdhury, P. K.; Halder, M.; Sanders, L.; Calhoun, T.; Anderson, J. L.; Armstrong, D. W.; Song, X.; Petrich, J. W. *J. Phys. Chem. B* **2004**, *108*, 10245.

(27) Ito, N.; Arzhantsev, S.; Heitz, M.; Maroncelli, M. *J. Phys. Chem. B* **2004**, *108*, 5771.

(28) Arzhantsev, S.; Ito, N.; Heitz, M.; Maroncelli, M. *Chem. Phys. Lett*. **2003**, *381*, 278.

(29) Ito, N.; Arzhantsev, S.; Maroncelli, M. *Chem. Phys. Lett*. **2004**, *396*, 83.

(30) Charkrabarty, D.; Hazra, P.; Chakraborty, A.; Seth, D.; Sarkar, N. *Chem. Phys. Lett*. **2003**, *381*, 697.

(31) Mandal, P. K.; Sarkar, M.; Samanta, A. *J. Phys. Chem. A* **2004**, *108*, 9048.

(32) Ammon, H. L. *J. Am. Chem. Soc*. **1973**, *17*, 7093.

(33) Gomaa, M. A.-M. *J. Chem. Soc., Perkin Trans. 1* **2002**, 341.

(34) Terazima, M.; Hara, T.; Hirota, N. *Chem. Phys. Soc.* **1995**, *246*, 577.

(35) Takeuchi, S.; Tahara, T. *J. Chem. Phys.* **2004**, *120*, 4768.

(36) Osawa, E.; Kitamura, K.; Yoshida, Z. *J. Am. Chem. Soc.* **1967**, *89*, 3814.

(37) Almeida, L. C. J.; Santos, P. S. *Spectrochim. Acta* **2002**, *58*, 3139.

(38) Kimura, Y.; Fukuda, M.; Fujisawa, T.; Terazima, M. *Chem. Lett*. **2005**, *34*, 338.

(39) See, e.g.: Reichardt, C. *Solvents and Solvents effects in Organic Chemistry*; VCH: Weinheim, Germany, 1988.

(40) Figueras, J. *J. Am. Chem. Soc*. **1971**, *93*, 3255.

(41) Yamaguchi, T.; Kimura, Y.; Hirota, N. *J. Phys. Chem. A* **1997**, *101*, 9050.

(42) Yamaguchi, T.; Kimura, Y.; Hirota, N. *J. Chem. Phys.* **1997** *107*, 4436.

(43) Yamaguchi, T.; Kimura, Y.; Hirota, N. *J. Chem. Phys.* **1998**, *109*, 9075.

(44) Yamaguchi, T.; Kimura, Y.; Hirota, N. *J. Chem. Phys.* **1998**, *109*, 9084.

(45) Morley, J. O.; Fitton, A. L. *J. Phys. Chem. A* **1999**, *103*, 11442.

(46) Nagasawa, Y.; Watanabe, A.; Ando, Y.; Okada, T. *J. Mol. Liq.* **2001**, *90*, 295.

(47) Chen, J.; Shen, D.; Wu, W.; Han, B.; Wang, B.; Sun, D. *J. Chem. Phys*. **2005**, *122*, 204508.

(48) Huddleston, J. G.; Wilauer, H. D.; Swatloski, R. P.; Visser, A. E.; Rogers, R. D. *Chem. Commun.* **1998**, *16*, 1765.

(49) Holbrey J. D.; Seddon, K. R. *J. Chem. Soc., Dalton Trans*. **1999**, 2133.

(50) Cammarata, L.; Kazarian, S. G.; Salter, P. A.; Welton, T. *Phys. Chem. Chem. Phys.* **2001**, *3*, 5192.

(51) Dupont, J.; Consorti, C. S.; Suarez, P. A. Z.; de Souza, R. F. *Org. Synth.* **2003**, *79*, 236.

(52) Marcus, Y. *Chem. Soc. Rev.* **1993**, *22*, 409.

(53) We assume that the value of AN cyclohexane is 0 because the empirical solvent parameters such as α, β, π^*, $E_T(30)$, donnor number, acidity, and basity are almost completely the same as those of *n*-hexane and *n*-heptane of which AN values are 0.[48]

(54) The Raman spectrum in [BPY][BF_4] was not measured due to strong fluorescence from the solvent.

(55) Headley, A. D.; Jackson, N. M. *J. Phys. Org. Chem*. **2002**, *15*, 52.

(56) Antony, J. H.; Mertens, D.; Dolle, A.; Wasserscheid, P.; Carper, W. R. *ChemPhysChem* **2003**, *4*, 588.

(57) Kolling, O. W. *Anal. Chem.* **1981**, *53*, 54.

(58) Kamlet, M. J.; Abboud, J.-L. M.; Abraham, M. H.; Taft, R. W. *J. Org. Chem.* **1983**, *48*, 2877.

(59) Ulstrup, J.; Jortner, J. *J. Chem. Phys.* **1975**, *63*, 4358.

(60) Sakaebe, H.; Matsumoto, H. *Electrochem. Commun.* **2003**, *5*, 594.

(61) Tokuda, H.; Hayamizu, K.; Ishii, K.; Susan, Md. A. B. H.; Watanabe, M. *J. Phys. Chem. B* **2004**, *108*, 16593.

(62) Huddleston, J. G.; Visser, A. E.; Reichert, W. M.; Willauer, H. D.; Broker, G. A.; Rogers, R. D. *Green Chem*. **2001**, *3*, 156.

(63) Gu, Z.; Brennecke, J. F. *J. Chem. Eng. Data.* **2002**, *47*, 339.

(64) Fredlake, C. P.; Crosthwaite, J. M.; Hert, D. G.; Aki, S. N. V. K.; Brennecke, J. F. *J. Chem. Eng. Data* **2004**, *49*, 954.

(65) Kim, Y.-J.; Matsuzawa, Y.; Ozaki, S.; Park, K. C.; Kim, C.; Endo, M.; Yoshida, H.; Masuda, G.; Sato, T.; Dresselhaus, S. D. *J. Electrochem. Soc.* **2005**, *152*, A710.

(66) Since there is a confusion of the reported values of the density of $[N(Et)_2(Me)(MetOEt)][(CF_3SO_2)_2N]$ in the literature (1.24 g cm^{-3} in ref 59 and 1.42 g cm^{-3} in the data sheet published from Nisshinbo Co.), we have measured the density by a density meter (Anton Paar: DMA4500), and the result was 1.41 g cm^{-3} at 25 °C.

(67) MacRae, E. G. *J. Phys. Chem.* **1957**, *61*, 562.

(68) According to the dielectric continuum model, the solvent polarizaility decreases ΔG as $\Delta G_P = [(\mu_g^2 - \mu_e^2)/(4\pi\epsilon_0 a^3)][(n^2 - 1)/(2n^2 + 1)] = A[(n^2 - 1)/(2n^2 + 1)]$, where n is the refractive index of the solvent, μ_g and μ_e are the dipole moments of the solute in the electronic ground and excited states, ϵ_0 is the dielectric constant of vacuum, and a is the radius of the solute molecule.[67,39] We have estimated the proportional constant of A empirically using the spectrum shift from supercritical ethane to cyclohexane, since in these solvents the solvent effect on the absorption peak mostly comes from the polarizability term. The absorption band centers are 18 420 cm^{-1} in cyclohexane and 19 465 cm^{-1} in ethane at $\rho_r = 1.4$, where ρ_r is the reduced density by the critical density of the solvent.[41] The refractive indices of these solvents are 1.43 and 1.17, respectively. As is discussed in the study by Yamaguchi et al.,[41] the intramolecular reorganization energy of PB is dependent on the solvent, which also affects the absorption band center. They have roughly estimated the term as $\omega_V\lambda_V = 400w_0 - 5\,200\,000$, and the subtraction of this term results in the spectra shift due to the ΔG term as 700 cm^{-1} from ethane at $\rho_r = 1.4$ to cyclohexane. Therefore A is estimated as ca. 10 000 cm^{-1}. According to the refractive index data of RTILs, we have estimated the effect is the largest in the solvent [BMIM]-[Cl] as +260 cm^{-1} relative to cyclohexane, which explains the larger absorption shift to some extent.